

Research Article

Experimental Characterization of 2×2 Electronically Reconfigurable Polarization Converter Unit Cells at X-Band

Biswarup Rana ¹, In-Gon Lee ¹, and Ic-Pyo Hong ²

¹Smart Natural Space Research Centre, Kongju National University, Cheonan 31080, Republic of Korea

²Department of Information and Communication Engineering, Kongju National University, Cheonan 31080, Republic of Korea

Correspondence should be addressed to Ic-Pyo Hong; iphong@kongju.ac.kr

Received 2 March 2021; Accepted 19 June 2021; Published 28 June 2021

Academic Editor: Symeon Nikolaou

Copyright © 2021 Biswarup Rana et al. This is an open access article distributed under the Creative Commons Attribution License, which permits unrestricted use, distribution, and reproduction in any medium, provided the original work is properly cited.

In this paper, an electronically reconfigurable polarization converter unit cell operating at X-band is proposed. The polarization converter unit cell consists of a passive patch, a phase shifter, and an active patch. There are two PIN diodes on the active patch. By switching the bias conditions of those PIN diodes, an electronically reconfigurable polarization converter is conceived. Both the passive and active patches are circular, and there are circular types of slots on both patches to enhance the operating bandwidth. To compensate for the capacitance introduced by PIN diodes, an equivalent capacitance structure is introduced on the active patch. 2×2 unit cells are designed to check the performance of the unit cell for polarization conversion applications. In addition, a novel type of experimental characterization technique is proposed to check the performance of polarization conversion using 2×2 unit cells. Two WR-90 waveguide sections, two rectangular to square sections, and a power supply are taken for the measurements. The rectangular to square waveguide transition section is designed in such a way so that 2×2 unit cells can be perfectly adjusted on the transition section and the performance of the 2×2 unit cells can be measured. The simulation results of the 8×8 array are also added to a miniaturized X-band horn antenna to check the performance of the overall array.

1. Introduction

In recent years, transmitarray is getting tremendous attention because of its simple structure, ease to fabricate, low cost, and very low loss compared to traditional phased array antennas [1–13]. Transmitarray is a promising candidate compared to reflectarray [14, 15] for reconfigurable polarization conversion of electromagnetic waves as there is no blocking element on the direction of propagating waves. Nowadays, polarization conversion of electromagnetic waves is getting considerable interest by researchers owing to their applications in the reduction of multipatch fading loss, providing double transmission channel for frequency reuses, reduction of radar cross section, etc. Polarization converters can provide the transformation of electromagnetic waves in different desired polarizations. A linearly polarized wave can be converted to its cross-polarized wave, or a linearly polarized wave can be converted to a circularly polarized wave by a polarization converter. There are different techniques by which a polarization

converter can be made such as anisotropy metasurfaces [16–18], frequency selective surface [19], meander line [20], and grid-plate [21, 22]. However, those structures are not reconfigurable. A polarization reconfigurable structure is very much desirable in the modern communication system. A reconfigurable polarization converter can be obtained by using PIN diodes [23], microelectromechanical systems (MEMS) [24], varactor diode, etc.

In this paper, a novel type of unit cell for reconfigurable polarization conversion by using two PIN diodes is proposed [25]. By changing the bias voltage of the PIN diode, a linearly polarized wave can be changed to its cross-polarized wave. Moreover, a novel type of measurement technique is proposed to measure the performance of the unit cell for polarization converted waves by simply rotating 90° one waveguide with respect to another waveguide. To the authors' best knowledge, such a measurement technique using 2×2 unit cells is not reported yet in the literature for polarization converter transmitarrays. Two WR-90 sections, two rectangular to square waveguide

sections, and a power source are used to measure the performance of the 2×2 unit cells.

The paper is organized as follows. In Section 2, the configuration of the unit cell is discussed. In Section 3, the configuration of 2×2 polarization reconfigurable unit cells is explained and the biasing lines for the 2×2 unit cells are presented. Two WR-90 waveguides, two rectangular to square waveguide transition sections, and a power supply are considered to measure the polarization converted beams. In Section 4, we present this one. The simulated results of radiation patterns with an X-band miniaturized horn antenna for the 8×8 transmitarray are presented in Section 5 to confirm the overall performance in the actual scenario. Lastly, a conclusion is added.

2. Configuration of Unit Cell

The cross-sectional view of the proposed unit cell is presented in Figure 1. Taconic RF-35 substrate having permittivity 3.5, loss tangent of 0.0018, and height of 1.52 mm is considered to design the unit cell. The total area of the unit cell is $15 \text{ mm} \times 15 \text{ mm}$. The unit cell is simulated with Ansys Electronics Desktop software. As shown in Figure 1, two Taconic RF-35 substrates are stacked together with a bonding film having a permittivity of 3.38, height of 0.1 mm, and loss tangent of 0.028. As shown in Figure 2(a), the upper patch is loaded with a circular slot to enhance the bandwidth of the operating frequency. It has two PIN diodes for polarization conversion operation. When PIN diode 2 as shown in Figure 2(a) is the "On" condition and PIN diode 1 is the "Off" condition, the waves get no polarization conversion. When the PIN diode 2 is "Off" condition and PIN diode 1 is "On" condition, the copolarized waves become cross-polarized waves and cross-polarized waves become copolarized waves. To compensate for the capacitance introduced by PIN diodes on the upper patch, an equivalent capacitance is conceived by introducing a very thin cured patch close to the circular patch. The PIN diodes are placed in such a way it can be biased using a single biasing line. Therefore, one PIN diode is always "On" condition irrespective of the biasing condition. The upper patch has an outer radius of 3.9 mm and an inner radius of 1.5 mm. The radius of the annular ring is 2.4 mm. The lower patch has the same inner and outer patch radius as the upper patch as shown in Figure 2(b). The lower patch is a passive patch which is connected through a metalized via hole to the upper patch. Table 1 shows the detail dimensions of the unit cell. As shown in Figure 1, the biasing lines are kept inside (on the bonding film) of the substrate to minimize the effect of biasing on the receiving and radiating patches. The ground plane of the proposed unit cell is sandwiched between the lower Taconic RF-35 substrate and the bounding film. There is one circular cut with a diameter of 0.7 mm on the ground plane so that the central via hole connecting the upper and lower patches does not connect with the ground plane.

Figures 3(a) and 3(c) show the induced surface current distributions for forward and reverse bias conditions for the transmitting patch. Figures 3(b) and 3(d) show the induced surface current distribution for forward and reverse bias

conditions for the receiving patch. The result shows two different radiating modes according to the PIN diode states (i.e., polarization conversion On state or Off state). For the forward bias condition, there is a current path from the center to the transmitting patch edge along the x -direction, which can radiate electromagnetic waves as a vertical polarization mode, as shown in Figure 3(a). In case of the reverse bias state, the current path is along the y -direction on the transmitting patch, which can radiate orthogonally polarized mode as a horizontal polarization.

3. Design of 2×2 Unit Cells with Bias Lines

The performance of the unit cell is essential for the overall performance of the transmitarray. It is very much desirable to characterize and verify the unit cell performance before fabricating the whole transmitarray. To do this, a 2×2 unit cell is considered instead of one unit cell. The unit cell area is $15 \text{ mm} \times 15 \text{ mm}$. To measure the performance of the unit cells, a rectangular to square waveguide is fabricated. Figure 4 shows the configuration of the 2×2 unit cell to be measured with WR-90 waveguide and rectangular to square waveguide transition. The total area for 2×2 elements is $70 \text{ mm} \times 70 \text{ mm}$ as shown in Figure 4. Two rows of a metalized via hole were conceived on the substrate so that the continuity of the waveguide can be maintained through the substrate. There are a total of three connection points on the top layer. Among them, two are for the connections to PIN diodes on the bias line and one line is for the ground plane. Figure 5 depicts the bias lines of the 2×2 unit cells. One ground plane connection point (Connection point 3) and another connection point (Connection point 1 or Connection point 2) are sufficient for the polarization conversion operation. Each connection point has a resistance of 200Ω and an induction of 1.4 nH so that it can suppress the bias line unwanted signals. The ground plane size is $50 \text{ mm} \times 50 \text{ mm}$. Figure 6 shows the equivalent circuit of the PIN diode. For the forward bias condition, L_1 and R_1 are 0.05 nH and 5.2Ω , respectively. L_2 , R_2 , and C_2 are 0.05 nH, $300 \text{ K}\Omega$, and 25 fF for reverse bias condition. Figure 7 shows the bottom view of the 2×2 unit cells. Figure 8 shows the fabricated top view and bottom view of the 2×2 unit cells.

4. Experimental Characterization of 4-Element Unit Cells with Waveguide

The schematic of the whole setup is presented in Figure 9. Two X-band rectangular waveguides WR-90, two rectangular to square waveguide transition sections, and a power source are used to measure the performance of the 2×2 unit cells. To measure the reflection and transmission coefficient for the same polarization, two WR-90 waveguides are kept in the same plane. However, one WR-90 is in a 90° rotating plane while measuring the transmission coefficient for the converted polarization. Convention X-band rectangular WR-90 waveguide has an opening area of $22.86 \times 10.16 \text{ mm}^2$. However, our fabricated polarization converter has a total area of $30 \times 30 \text{ mm}^2$. The lowest order cutoff frequency of the

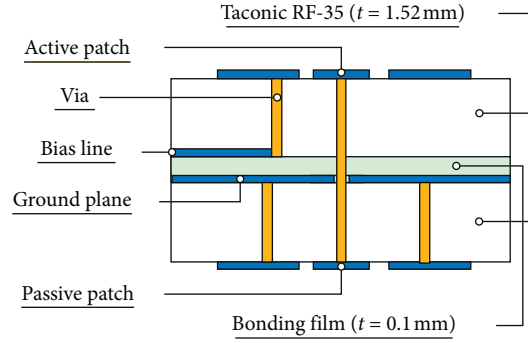


FIGURE 1: Cross-sectional view of the proposed unit cell.

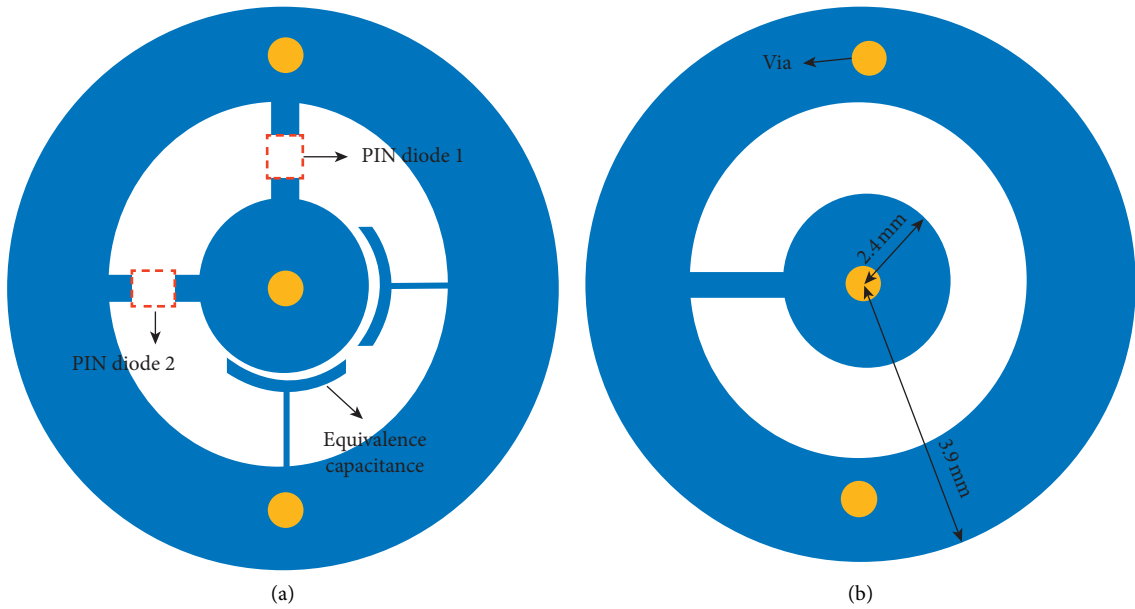


FIGURE 2: (a) Top view of the proposed unit cell; (b) bottom view of the proposed unit cell.

TABLE 1: Main features of the unit cell.

Parameter	Unit/description
Unit cell size	15 mm × 15 mm
Outer patch diameter	7.8 mm
Inner patch diameter	4.8 mm
Substrate	Taconic RF-35 ($\epsilon_r = 3.5$, $\tan\delta = 0.0018$, $h = 1.52$ mm)
Bonding film	$\epsilon_r = 3.38$, $\tan\delta = 0.028$, $h = 0.1$ mm
Dimeter of connecting via	0.4 mm
Diameter of bias via	0.4 mm
Ground plane opening diameter	0.7 mm
PIN diode	MACOM MA4GP907
Annular ring diameter	4.8 mm

30×30 mm² section is 4.99 GHz, and the next lower order cutoff frequency is 6.24 GHz. However, the rectangular to square waveguide section is very small and it does not prevent the propagation of TE₁₀ mode of the WR-90 waveguide within the rectangular to square transition sections. We have optimized the rectangular to square waveguide sections so that the TE₁₀ mode can propagate within the rectangular to square waveguide without any significant

attenuation. Thus, the rectangular to square sections do not affect the performance of the measurement technique. To measure the performance of the 2×2 unit cells, a rectangular to square waveguide transition section was fabricated. Figure 10 shows the fabricated transition section with the waveguide WR-90 and 2×2 polarization converter unit cells. The simulated and measured transmission and reflection coefficients of rectangular to the square waveguide

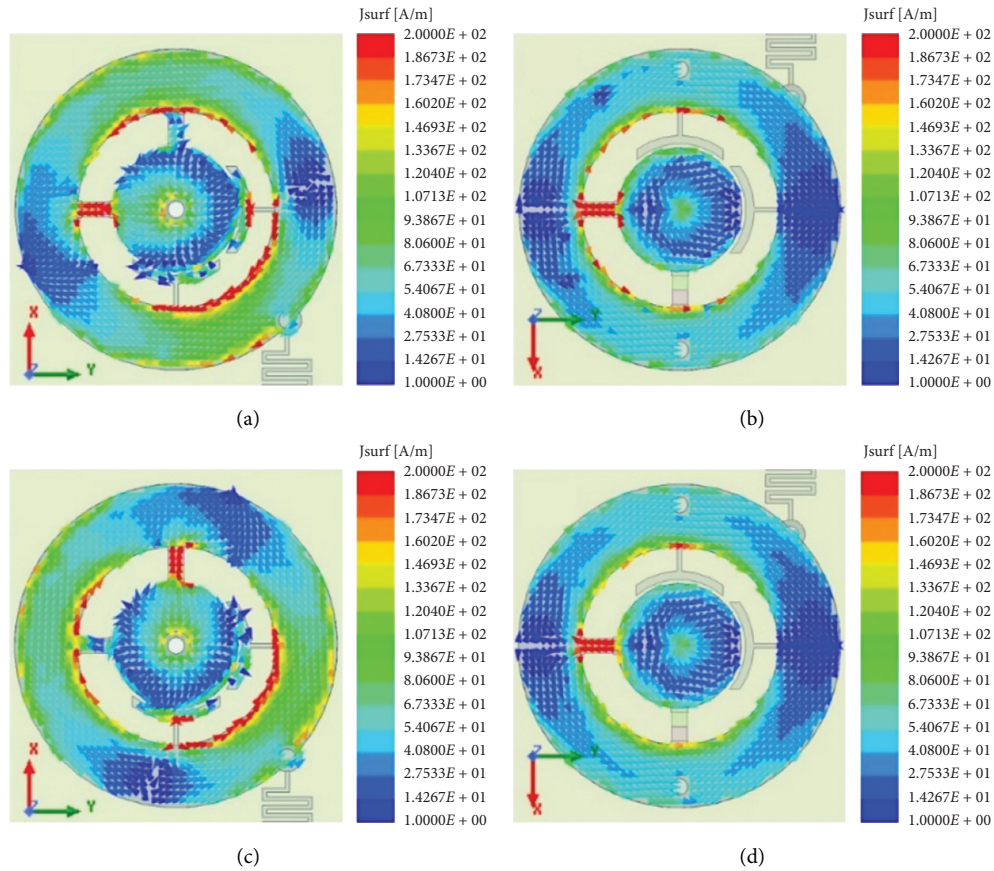


FIGURE 3: Simulated results for induced surface current distributions for different diode state: (a) transmitting patch on forward bias, (b) receiving patch on forward bias, (c) transmitting patch on reverse bias, and (d) receiving patch on reverse bias.

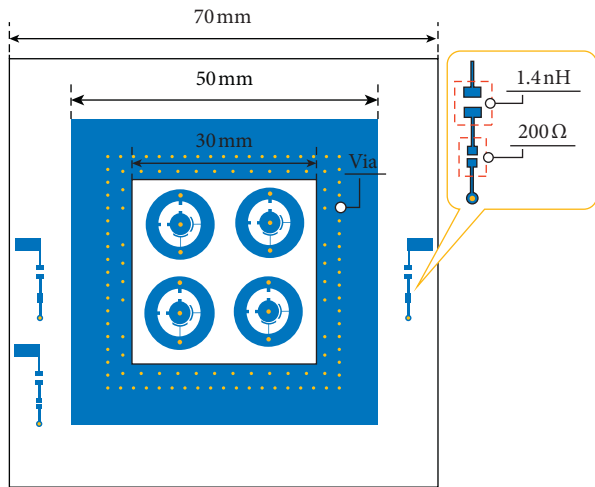


FIGURE 4: Top view of the 2×2 proposed unit cell.

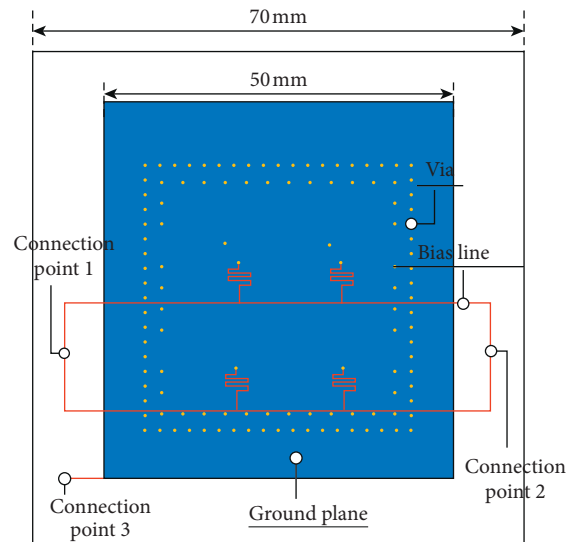


FIGURE 5: Biasing line view of the 2×2 proposed unit cell.

are depicted in Figure 11. It is observed that the performances of the rectangular to the square waveguide are very satisfactory within the X-band. The transmission coefficients and reflection coefficients of the proposed 2×2 unit cells for the copolarization wave are shown in Figure 12. Figure 13 shows the simulated and measured transmission and reflection coefficients for the polarization converted waves.

There is a good match between the simulated and measured results for both copolarization waves and polarization converted waves. A simulated and measured -3 dB bandwidths were 250 MHz (9.0 GHz–9.25 GHz) and 320 MHz (8.98 GHz–9.30 GHz) for the copolarization waves, respectively. Figure 13 shows the simulated and measured

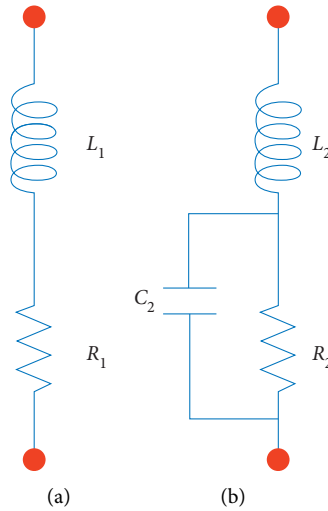


FIGURE 6: Equivalent circuit of the PIN diode: (a) for the forward bias condition and (b) for reverse bias condition.

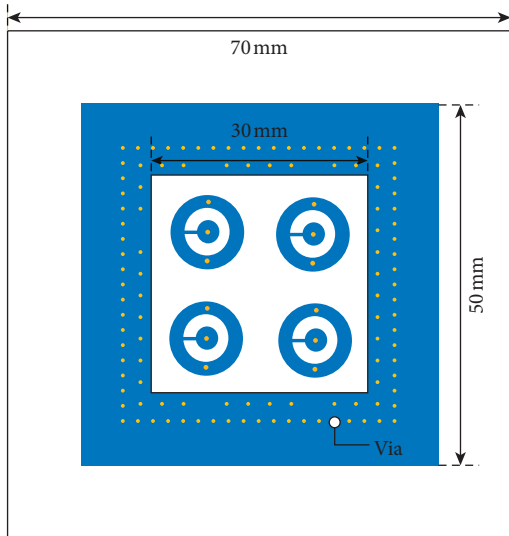


FIGURE 7: Bottom view of the 2×2 proposed unit cell.

transmission and reflection coefficients for the polarization converted waves. A simulated and measured -3 dB bandwidths were 350 MHz (9.0 GHz–9.35 GHz) and 260 MHz (9.02 GHz–9.28 GHz) for the polarization converted waves, respectively. There is a good match between the simulated and measured results for both copolarization waves and polarization converted waves.

5. Miniaturized Horn Antenna with 8×8 Transmitarray

A miniaturized horn antenna was considered to check the performance of the 8×8 array of the proposed unit cell. The focal length to diameter ratio (F/D) was 0.3 in this study. Figure 14 shows the simulation setup for the whole system. The simulated radiation pattern for the copolarization state is given in Figure 15, and the radiation pattern for the polarization converted state is depicted in Figure 16.

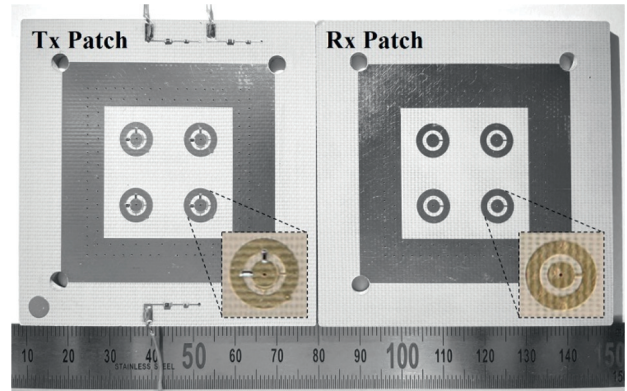


FIGURE 8: Fabricated top view and bottom view of the 2×2 proposed unit cells for polarization conversion.

The miniaturized horn was designed with Ansys Desktop software, and a maximum directivity of 11.2 dB was observed. The maximum directivity of the 8×8 transmitarray with miniaturized horn is 9.2 dB with no polarization conversion state as shown in Figure 15. The co-to-cross polarization differences at $\theta = 0^\circ$ are 22.7 dB and 23.5 dB for the E-plane and H-plane, respectively. And the maximum directivity for polarization converted waves is 10.3 dB as shown in Figure 16. The co-to-cross polarization differences for E-plane and H-plane at $\theta = 0^\circ$ are 14.5 dB and 14.3 dB, respectively. The sidelobe level of the miniaturized horn antenna can be affected by the 8×8 transmit array. When there was no 8×8 transmitarray, the sidelobe level of the miniaturized horn antenna was significantly less. The dominant factor, which can affect the sidelobe level, is the phase delay of each unit cell in the transmitarray. To reduce the sidelobe level, the phase compensation technique can be considered, but that was not our objective in this paper. With the introduction of the 8×8 transmit array, the sidelobe level of the horn antenna for both copolarization and converted polarization with the 8×8 transmitarray was high as shown in Figures 15 and 16.

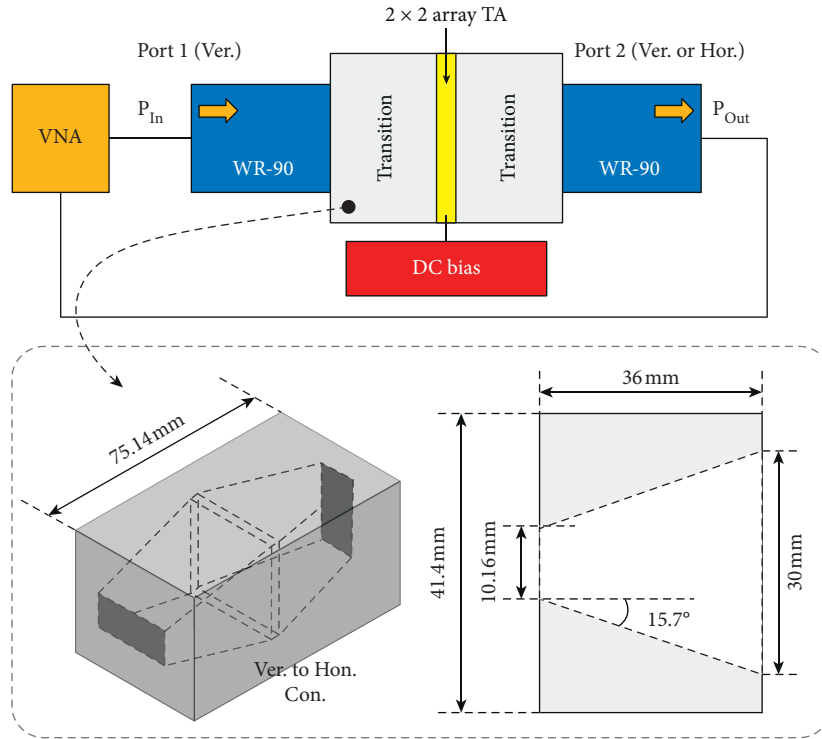


FIGURE 9: The geometry of the waveguide with transition section.

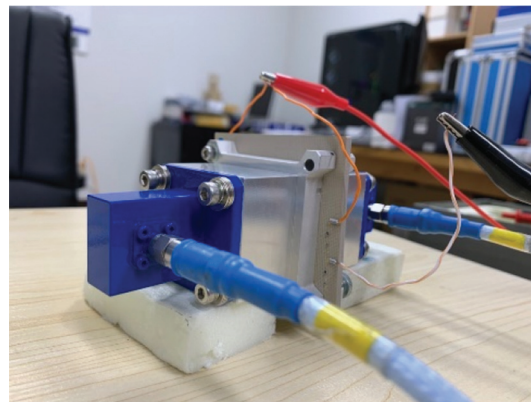


FIGURE 10: Waveguide setup with 2×2 unit cells.

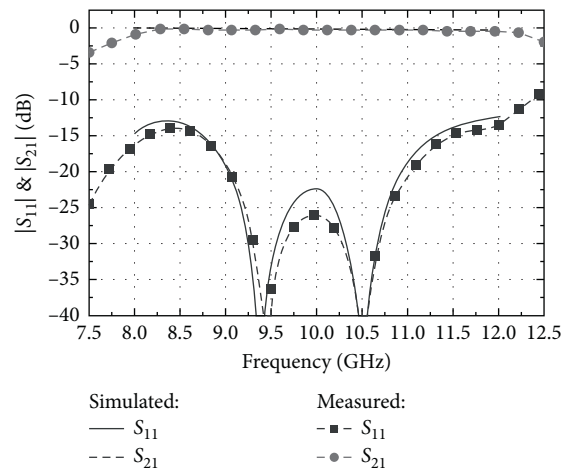


FIGURE 11: Magnitudes of S_{11} and S_{21} at transition section.

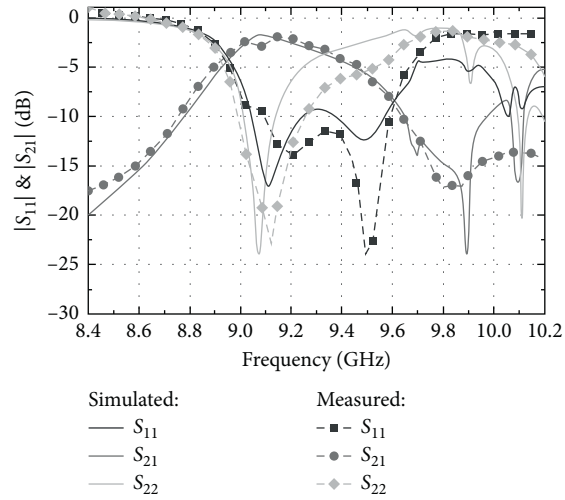


FIGURE 12: Magnitude of S_{11} , S_{21} , and S_{22} with 2×2 unit cell for copolarization.

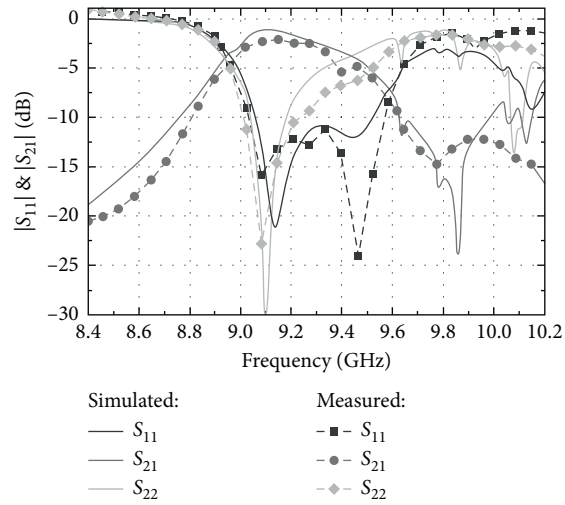


FIGURE 13: Magnitude of S_{11} , S_{21} , and S_{22} with 2×2 unit cell for polarization converted waves.

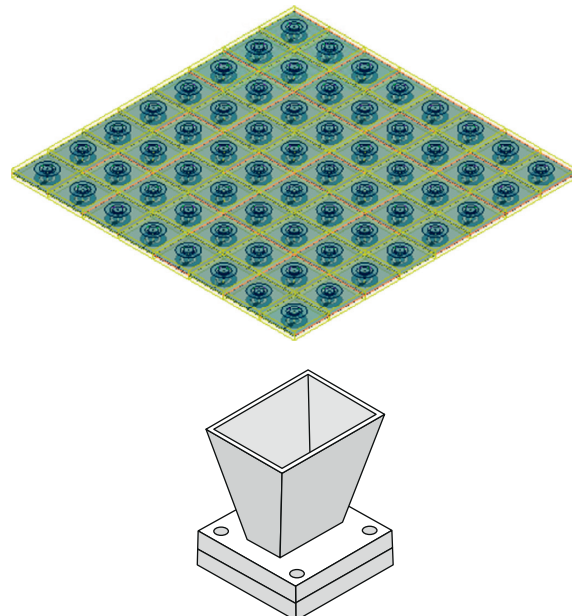


FIGURE 14: Simulation setup for an 8×8 array with miniaturized horn antenna.

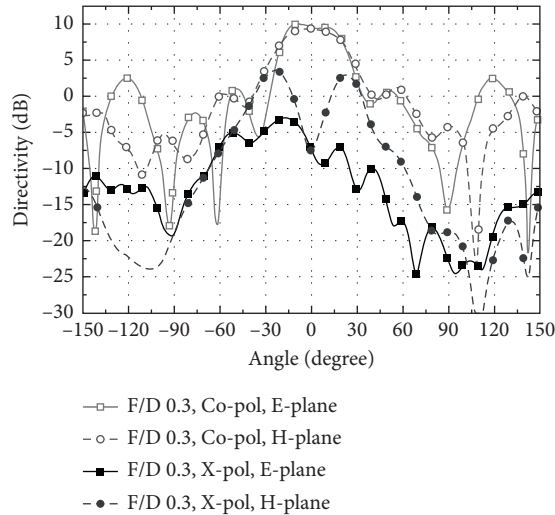


FIGURE 15: E-plane and H-plane patterns for the no polarization conversion state at 9.25 GHz.

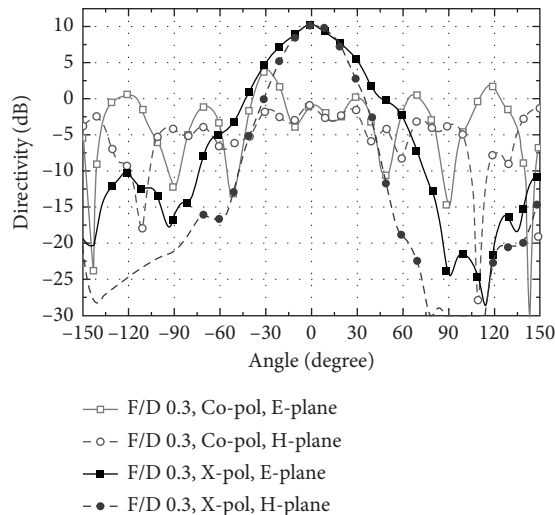


FIGURE 16: E-plane and H-plane pattern for the polarization converted state at 9.25 GHz.

6. Conclusions

In this paper, a new type of unit cell for polarization conversion is presented. A new method is proposed using X-band WR-90 wave and rectangular to square waveguide transition section to measure the performance of the unit cell for polarization conversion. By changing the bias voltage of the PIN diodes of the unit cells, the polarization conversion can be achieved electronically. The proposed method described here can be applied to any unit cell to check the performance initially without fabricating the whole transmitarray. An 8×8 unit was considered with an X-band miniaturized horn antenna to check the performance of the overall array. Satisfactory results were observed for the 8×8 array.

Data Availability

No data were used to support this study.

Conflicts of Interest

The authors declare that there are no conflicts of interest regarding the publication of this paper.

Acknowledgments

This research was supported by the Basic Science Research Program (2020R111A3057142) and the Priority Research Centers Program (2019R1A6A1A03032988) through the National Research Foundation of Korea.

References

- [1] A. Clemente, L. Dussopt, R. Sauleau, P. Potier, and P. Pouliguen, "1-bit reconfigurable unit cell based on PIN diodes for transmit-array applications in X-band," *IEEE Transactions on Antennas and Propagation*, vol. 60, no. 5, pp. 2260–2269, 2012.

- [2] A. Clemente, L. Dussopt, R. Sauleau, P. Potier, and P. Pouliguen, "Wideband 400-element electronically reconfigurable transmitarray in X band," *IEEE Transactions on Antennas and Propagation*, vol. 61, no. 10, pp. 5017–5027, 2013.
- [3] M. Wang, S. Xu, F. Yang, and M. Li, "Design and measurement of a 1-bit reconfigurable transmitarray with sub-wavelength H-Shaped coupling slot elements," *IEEE Transactions on Antennas and Propagation*, vol. 67, no. 5, pp. 3500–3504, 2013.
- [4] W. Pan, C. Huang, X. Ma, B. Jiang, and X. Luo, "A dual linearly polarized transmitarray element with 1-bit phase resolution in X-band," *IEEE Antennas and Wireless Propagation Letters*, vol. 14, pp. 167–170, 2015.
- [5] C. Huang, W. Pan, X. Ma, and X. Luo, "1 bit reconfigurable circularly polarized transmit-array in X Band," *IEEE Antennas and Wireless Propagation Letters*, vol. 14, pp. 167–170, 2015.
- [6] P. Padilla, A. Muñoz-Acevedo, M. Sierra-Castañer, and M. Sierra-Pérez, "Electronically reconfigurable transmitarray at Ku band for microwave applications," *IEEE Transactions on Antennas and Propagation*, vol. 58, no. 8, pp. 2571–2579, 2010.
- [7] J. Lau and S. V. Hum, "Analysis and characterization of a multipole reconfigurable transmitarray element," *IEEE Transactions on Antennas and Propagation*, vol. 59, no. 1, pp. 70–79, 2011.
- [8] J. Y. Lau and S. V. Hum, "Reconfigurable transmitarray design approaches for beamforming applications," *IEEE Transactions on Antennas and Propagation*, vol. 60, no. 12, pp. 5679–5689, 2012.
- [9] M. Frank, F. Lurz, R. Weigel, and A. Koelpin, "Electronically reconfigurable 6×6 element transmitarray at K-band based on unit cells with continuous phase range," *IEEE Antennas and Wireless Propagation Letters*, vol. 18, no. 4, pp. 5679–5689, 2012.
- [10] B. D. Nguyen and C. Pichot, "Unit-cell loaded with PIN diodes for 1-bit linearly polarized reconfigurable transmitarrays," *IEEE Antennas and Wireless Propagation Letters*, vol. 18, no. 1, pp. 98–102, 2019.
- [11] L. Di Palma, A. Clemente, L. Dussopt, R. Sauleau, P. Potier, and P. Pouliguen, "Experimental characterization of a circularly polarized 1 bit unit cell for beam steerable transmitarrays at ka-band," *IEEE Transactions on Antennas and Propagation*, vol. 67, no. 2, pp. 1300–1305, 2019.
- [12] J. R. Reis, M. Vala, and R. F. S. Caldeirinha, "Review paper on transmitarray antennas," *IEEE Access*, vol. 7, pp. 94171–94188, 2019.
- [13] D. McGrath, "Planar three-dimensional constrained lenses," *IEEE Transactions on Antennas and Propagation*, vol. 34, no. 1, pp. 46–50, 1986.
- [14] E. Carrasco, M. Barba, and J. A. Encinar, "X-band reflectarray antenna with switching-beam using PIN diodes and gathered elements," *IEEE Transactions on Antennas and Propagation*, vol. 60, no. 12, pp. 5700–5708, 2012.
- [15] M. Riel and J.-J. Laurin, "Design of an electronically beam scanning reflectarray using aperture-coupled elements," *IEEE Transactions on Antennas and Propagation*, vol. 55, no. 5, pp. 1260–1266, 2007.
- [16] H. L. Zhu, S. W. Cheung, K. L. Chung, and T. I. Yuk, "Linear-to-circular polarization conversion using metasurface," *IEEE Transactions on Antennas and Propagation*, vol. 61, no. 9, pp. 4615–4623, 2013.
- [17] X. Gao, X. Han, W.-P. Cao, H. O. Li, H. F. Ma, and T. J. Cui, "Ultrawideband and high-efficiency linear polarization converter based on double V-shaped metasurface," *IEEE Transactions on Antennas and Propagation*, vol. 63, no. 8, pp. 3522–3530, 2015.
- [18] Y. Li, J. Zhang, S. Qu et al., "Achieving wide-band linear-to-circular polarization conversion using ultra-thin bi-layered metasurfaces," *Journal of Applied Physics*, vol. 117, no. 4, 2015.
- [19] M. Euler, V. Fusco, R. Cahill, and R. Dickie, "325 GHz single layer sub-millimeter wave FSS based split slot ring linear to circular polarization convertor," *IEEE Transactions on Antennas and Propagation*, vol. 58, no. 7, pp. 2457–2459, 2010.
- [20] M.-A. Joyal and J.-J. Laurin, "Analysis and design of thin circular polarizers based on meander lines," *IEEE Transactions on Antennas and Propagation*, vol. 60, no. 6, pp. 3007–3011, 2012.
- [21] C. Dietlein, A. Luukanen, Z. Popovi, and E. Grossman, "A W-band polarization converter and isolator," *IEEE Transactions on Antennas and Propagation*, vol. 55, no. 6, pp. 1804–1809, 2007.
- [22] W. A. Shiroma, S. C. Bundy, S. Hollung, B. D. Bauernfeind, and Z. B. Popovic, "Cascaded active and passive quasi-optical grids," *IEEE Transactions on Microwave Theory and Techniques*, vol. 43, no. 12, pp. 2904–2909, 1995.
- [23] W. Li, S. Xia, B. He et al., "A reconfigurable polarization converter using active meta surface and its application in horn antenna," *IEEE Transactions on Antennas and Propagation*, vol. 64, no. 12, pp. 5281–5290, 2016.
- [24] T. Debogovic, J. Bartolic, and J. Perruisseau-Carrier, "Dual-polarized partially reflective surface antenna with MEMS-based beam width reconfiguration," *IEEE Transactions on Antennas and Propagation*, vol. 62, no. 1, pp. 228–236, 2014.
- [25] B. Rana, I.-G. Lee, and I.-P. Hong, "Experimental characterization of 2×2 electronically reconfigurable 1 bit unit cells for a beamforming transmitarray at X band," *Journal of Electromagnetic Engineering and Science*, vol. 21, no. 2, pp. 153–160, 2021.